

Front page

Exam information

NFYA09004E - Nanoscience Thesis 60 ECTS, Niels Bohr
Institute - Contract:134694 (Christos Drakos)

Handed in by

Christos Drakos
hrk840@alumni.ku.dk

Exam administrators

Eksamensteam, tel 35 33 64 57
eksamen@science.ku.dk

Assessors

Heloisa Nunes Bordallo
Examiner
bordallo@nbi.ku.dk
☎ +4535321215

Jan Skov Pedersen
Co-examiner
jsp@chem.au.dk

Hand-in information

Title: Investigating the polymorphic structure of cocoa butter

Title, english: Investigating the polymorphic structure of cocoa butter

The sworn statement: Yes

Does the hand-in contain confidential material: No



Investigating the polymorphic structure of Cocoa Butter

Chris Drakos

Supervisor: Heloisa Bordallo

Co-Supervisor: Hery Mitsutake

Submitted on: 20 May 2023

Name of department: Niels Bohr Institute

Author(s): Chris Drakos

Title and subtitle: Investigating the polymorphic nature of Cocoa Butter

Topic description: Using thermal analysis alongside X-Ray scattering techniques the polymorphism of Cocoa Butter is investigated.

Supervisor: Heloisa Bordallo
Co-Supervisor: Hery Mitsutake

Submitted on: 20 May 2023

Grade: [X]

Number of study units:

2 3

Number of characters: [XXX]

Table of contents

1. ABSTRACT	4
2. INTRODUCTION	5
3. MATERIALS AND METHODS	7
4. RESULTS	10
4.1 DSC data	10
4.2 SAXS data	15
4.3 WAXS data	20
4.4 Crystallization process	25
5. DISCUSSION AND CONCLUSION	27
6. PERSPECTIVES	29
7. BIBLIOGRAPHY	30

1. Abstract

Polymorphism has been observed in cocoa butter in numerous experiments, giving rise to many protocols on how to create each form. Here we use the protocol created by Bresson (et al. 2011) as a guide and look deeper in the crystallization process and the effect of varying the heating/cooling rates through DSC and SAXS/WAXS. Cocoa Butter can crystallize in 6 different forms. We have attained data for three forms (Form II, III, IV). For all forms the effect of the heating/cooling rates was observed with DSC and further investigated with X-rays. Data shows different forms created alongside the desired one. Form IV seems to exist in combination with the other two forms. A thermodynamic approach was also used where the Gibbs free energy was calculated to better understand the internal transitions that might occur. Form IV seems to be able to transition to both Form II and III while Form III and II seem to exhibit a monotropic relationship meaning Form II can transition to Form III spontaneously and not the other way around.

2. Introduction

Matter exists in multiple forms, two of them are liquid and solid. When a liquid is cooled atoms tend to come together and form clusters (Giocovazzo et al. 2011) resulting in a phase transition: liquid to solid. Solids are observed as rigid structures with tightly packed atoms and strong bonds among them. The tendency of solids to arrange in an ordered manner due to the lower energy required results in what is called a crystalline state, The difference between a solid and a crystal structure comes in the ability of repetition that is present in a crystal. If you move along a solid the bonds and distances between atoms are to an extent random. On the other hand, in a crystal periodicity is observed. Smaller parts, called unit cells, can be found repeatedly throughout the whole structure making up the whole system. The unit cell is the smallest volume that can be used to describe our crystal structure and can also be extended to form the 14 Bravais lattices which make the identification and grouping of the crystalline forms more efficient. Most materials crystallize in a single way and the advances in X-ray technology have enabled studying the structures and the creation of an extensive database by many researchers through the years. However, some materials exhibit a unique feature called polymorphism.

Polymorphism is the ability of a material to crystallize in two or more ways. The importance of this ability lies in the fact that the same compounds, with the only difference being the arrangement in space, exhibit different physicochemical characteristics such as melting temperature, crystal shape and different vibrational transitions (Nogueira et al. 2020). This is important in many fields i.e., pharmaceuticals, food production and explosives. A drug, for example, changing its crystal structure due to poor handling and resulting in poisoning rather than curing can be an ampt example of the importance in examining the polymorphic nature of materials.

Cocoa butter, the material under investigation, is of polymorphic nature and one of the main ingredients for manufacturing chocolate. Since it is a fat, it is mostly consisting of triglycerides (Loisel et al.1998). The components that make up the triacylglycerols (TAGs) and mainly appear in the CB are oleic (O), stearic (S), and palmitic (P) acid. These individual components exhibit polymorphic nature of their own and have many ways of folding and organizing in space (Bayés-García et al. 2013). The complexity of CB's crystallization has been the focus of a lot of research. Researchers even debated whether the six forms that have been observed are all individual and unique and not an amalgamation of different forms giving rise to observable features (Wille et al. 1966). The notation that is used in this thesis to distinguish between the different forms is the one that Wille and Lutton established which incorporates the roman numerals. So, the six forms are notated as: Form I, Form II, Form III, Form IV, Form V, Form VI.

Since CB is a main ingredient for making chocolate, the food industry has focused on finding protocols that describe the way to acquire the desired crystal form and how to keep the crystals from changing and the product showing signs of deterioration. The main characteristics that a product needs to exhibit are that of gloss, snap, and color. It is established that form V gives the best results for these characteristics. Since the products may undergo various conditions following the manufacturing process (extended shelf life, inappropriate storage, high temperatures) the crystal structure is influenced in the long run. The main problem that occurs is the so-called "fat bloom" (the white spots that sometimes appear in chocolate products) where form V crystals start to melt and form VI are created (Sato et al. 2013).

As cited before, different polymorphic forms have different melting points. The different melting ranges and points are shown in table 1. In Bresson’s article their results are compared to Wille and Lutton work. Form I, according to Bresson has an onset melting point from 11.5 – 12.5°C and according to Wille and Lutton a peak melting temperature of 17.3°C. Form II has an onset melting point of 16.5 – 18°C and a peak melting temperature of 23.3°C. Form III range is 19.5 - 21.5°C and peak of 25.5°C, while form IV has 25.5 – 28°C and peak of 27.5°C. Form V ‘s onset point is 30.5 – 32°C and its peak can be found at 33.9°C. Lastly form VI has a melting point of 33.5 – 35.5°C and peak at 36.3°C (Table 1).

	Form I	Form II	Form III	Form IV	Form V	Form VI
Bresson	11.5-12.5°C	16.5-18°C	19.5-21.5°C	25.5-28.0°C	30.5-32.0°C	33.5-35.5°C
Wille and Lutton	17.3°C	23.3°C	25.5°C	27.5°C	33.9°C	36.3°C

Table 1: Temperature ranges and peaks for the polymorphs of the cocoa butter (Bresson et al. 2011).

This work is focused on investigating Form II, III and IV. Bresson protocol was used for the isolation and studying of the individual forms. Figure 1 illustrates the process for acquiring the crystal structures directly from melted cocoa butter. It should be noted that although the crystals may melt at lower temperatures (Table 1), we reached 60°C to ensure the complete melt of all crystal structures and the erasure of crystal memory, a phenomenon that is present in CB and affects the crystallization process (Van Langevelde et al. 2001). The methods used for studying the forms are Differential Scanning Calorimetry (DSC), for their thermal properties, and X-ray scattering both at small and wide angles (SAXS and WAXS) to extract internal structure information.

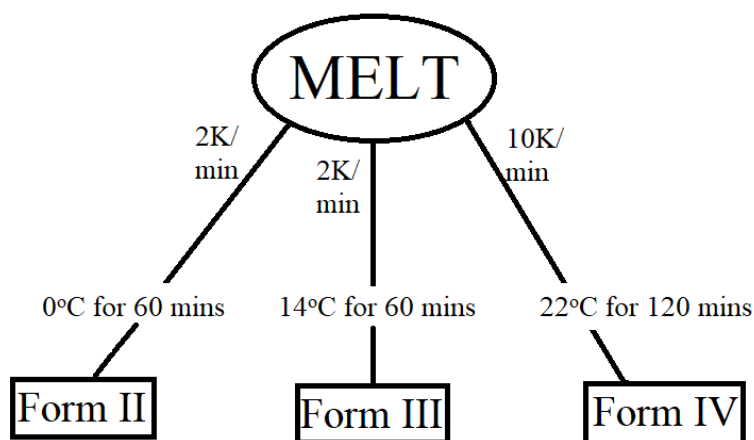


Figure 1: The protocol followed by Bresson (1). Melt is the point after the sample has been heated to 60 °C and kept there for ten minutes. After that the heating rates are presented and the temperature that the sample is kept to crystallize in the desired form.

3. Materials and Methods

To investigate the phase transitions of our cocoa butter polymorphs, one of the methods that were used is the Differential Scanning Calorimetry (DSC). This method uses the heat flow as an indicator of phase changes. The melting process is an endothermic process i.e., energy is necessary to melt the crystals. On the other hand, the formation of a crystal system is an exothermic process; it releases energy, and no energy is necessary for the process to be completed. For a DSC measurement, a reference (empty crucible) is placed on top of a small heating plate along with our sample inside a small chamber (Figure 2). The difference in temperature between the reference and the sample should always be zero. When the crystals in our sample start to melt more heat is required for the melting to be completed while the reference doesn't need any extra heat. The difference in this heat flow is recorded by the instrument. During the crystallization, the sample releases energy as the crystals start to form and less heat is required to be provided in relation to the reference to keep the temperature difference at zero. These heat flow differences are used to determine the phase transitions temperatures (Menczel & Grebowicz et al. 2023)

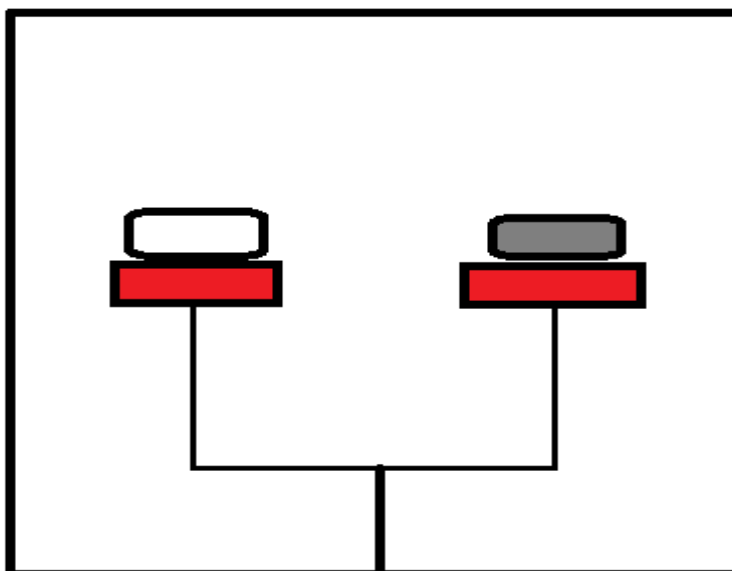


Figure 2: The chamber of a DSC instrument. On the left the empty crucible used as a reference and on the right the loaded crucible containing our sample.

3 mg of CB has been hermetically sealed in aluminium pans ideal for DSC measurements. Following the process shown in Figure 1, we made measurements for three forms: II, III, and IV. Before every measurement we bring the sample to a temperature of 60°C and keep it there for 10

minutes so that all crystals melt, and erase memory effects. Then for each form there is a different temperature program used: Form II is cooled from 60°C down to 0°C with a cooling rate of 2K/min and kept there for one hour. Form III is cooled by 2K/min and brought to 14°C where it is kept for one hour. Form IV is cooled by 10 K/min and kept for two hours at 22°C. All measurements have been recorded in two cycles to check the reproducibility of the protocol. As such, one cycle starts as soon as we start cooling to the specific temperatures, from 60°C, and then heating up to 60°C again. The instrument used for the measurements is a Netzsch DSC 214 with nitrogen gas flow of 40 mL/min purge 2 MFC and 60mL/min protective MFC.

Based on the properties of X-rays (highly penetrative and small wavelength), they are suited for internal structure investigation. Thinking about X-ray photons as waves, with specific wavelength and amplitude, we can imagine the waves travelling and come into contact with our sample. On contact, some of them are reflected from the surface while others penetrate a bit further, a distance we call d representing the crystal's spacings, and then reflected back out of the sample. The waves that were reflected from different spacings then interact with each other resulting in constructive or destructive interference. The type of interference can be determined through Bragg's Law, Eq.1

$$n\lambda=2d\sin\theta \quad (\text{Eq.1})$$

with n the diffraction order, λ the wavelength, d crystal spacings and θ the scattering angle, where if the equation is satisfied constructive interference occurs. Destructive interference gives minimal

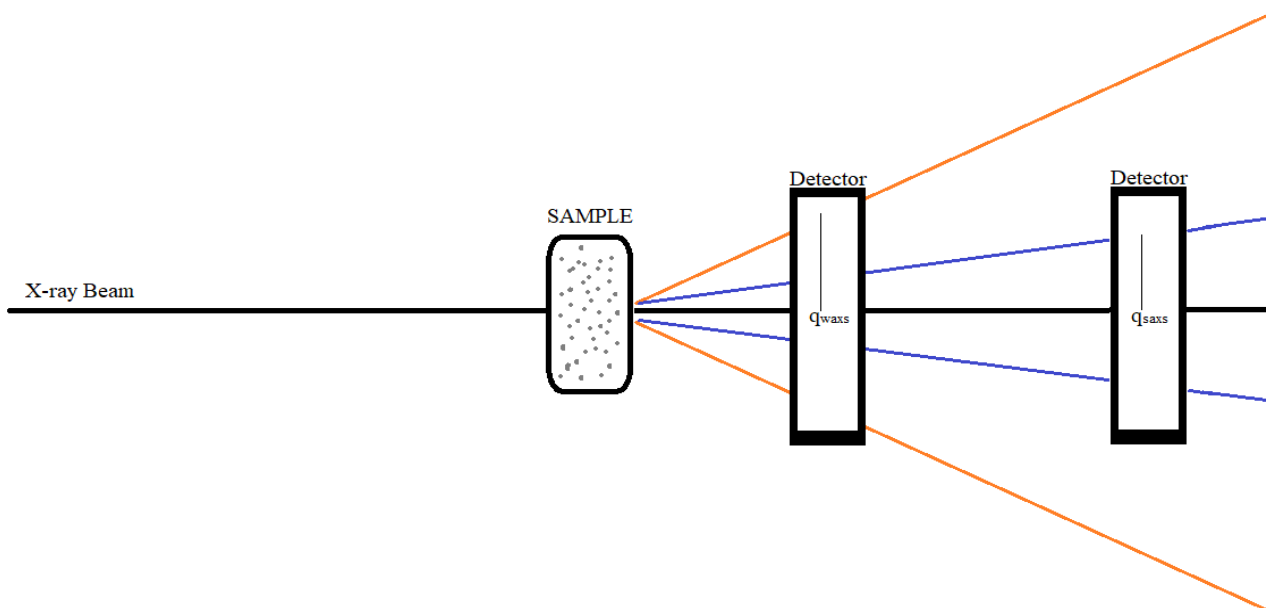


Figure 3: SAXS and WAXS setup representation. Changing the distance between the sample and the detector enables us to probe different q values which represent different internal spacings of the material under investigation. Bigger q values (WAXS) represent small spacings (in our case 3-5 Å) while smaller q values represent bigger internal spacings (40-50 Å).

intensity while constructive results in a measurable signal on our detector. The recorded intensity pattern is expressed through equation 2, where 2θ is the scattering angle.

$$q=(4\pi\sin\theta)/\lambda \quad (\text{Eq.2})$$

Combining Bragg's Law (Eq.1) and the function for q (Eq.2), we end up with a simple equation;

$$d=2\pi/q \quad (\text{Eq.3})$$

This equation combines the detector's readings to the internal structure of our sample. A peak at a specific q translates to specific crystal spacings. In our case both small-angle and wide-angle scattering methods are used. Figure 3 shows the setup and difference between SAXS and WAXS. Note the difference between the SAXS and WAXS is the distance from the sample to the detector. For SAXS the sample is further away from the detector compared to WAXS probing different internal spacings.

For the X-ray measurements we used a copper cell, which guarantees proper heat flow, to enclose a sufficient amount of CB and a Peltier stage suited for temperature control. We measured the intensity of the scattered X-rays and the angle in which they were detected. The instrument used is a Nano-inXider by Xenocs with a Cu source at 8KeV and wavelength of 1.54 Å.

Measurements were also done to investigate the effect of the heating and cooling rate and how it affects the crystallization. For the three forms (II, III, IV) the figure 1 process was followed again but this time with heating/cooling rates of 5 and 10K/min for Forms II and III for both DSC and X-ray measurements, while Form IV was recorded with 5K/min during the X-ray runs, due to long acquisition times required.

4. RESULTS

4.1 DSC data

DSC curves for Form II can be seen in figures 4 - 6. The protocol suggests a cooling rate of 2K/min until 0°C and afterwards an isothermal rest for 1 hour. Measurements were also made with heating/cooling rates of 5K/min and 10K/min. One common feature on all our curves is the big peak at approximately 32°C. This is the initial heating to 60°C as mentioned before to avoid any crystal memory effects. The 32°C melting point can be associated with Form V which might have formed through solid-solid transitions when the sample was left at room temperature between the measurements. Figure 4 illustrates the curves for 2K/min. After fitting the heating parts with OriginPro2020, there are indications that Form III and IV crystals co-exist with crystals of Form II. Figure 5 shows the DSC measurements for 5K/min and Figure 6 for 10K/min.

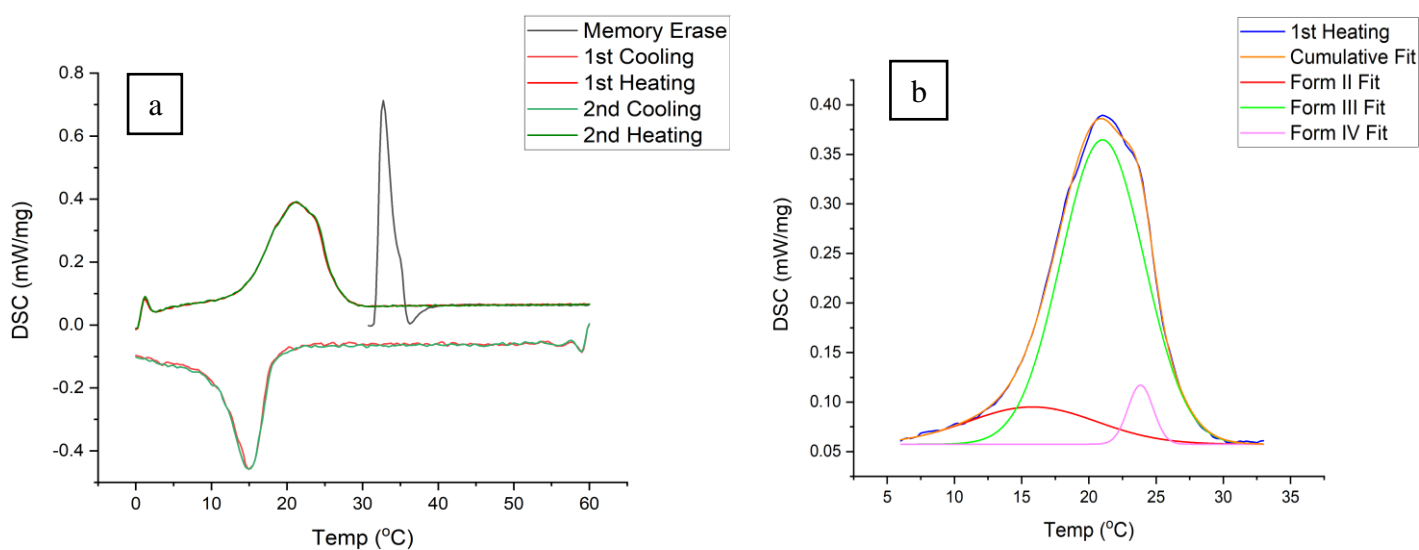


Figure 4: a) DSC curves for Form II with a cooling/heating rate of 2K/min. The black line is the first heating at 60°C after our sample has been at room temperature for a couple of days. The melting range indicates that they are crystals of Form V melting. The temperature ranges on both heating steps overlap and indicate the creation of Form II crystals. b) Fitted DSC data showing the creation of more than Form II crystals. The red peak appears at approximately 15.8°C indicative of Form II melting range. The green fit is indicative of Form III with a peak at 21°C. The purple peak is situated at ~24.8°C close to the melting range of Form IV. The orange peak is the cumulative fit of the three.

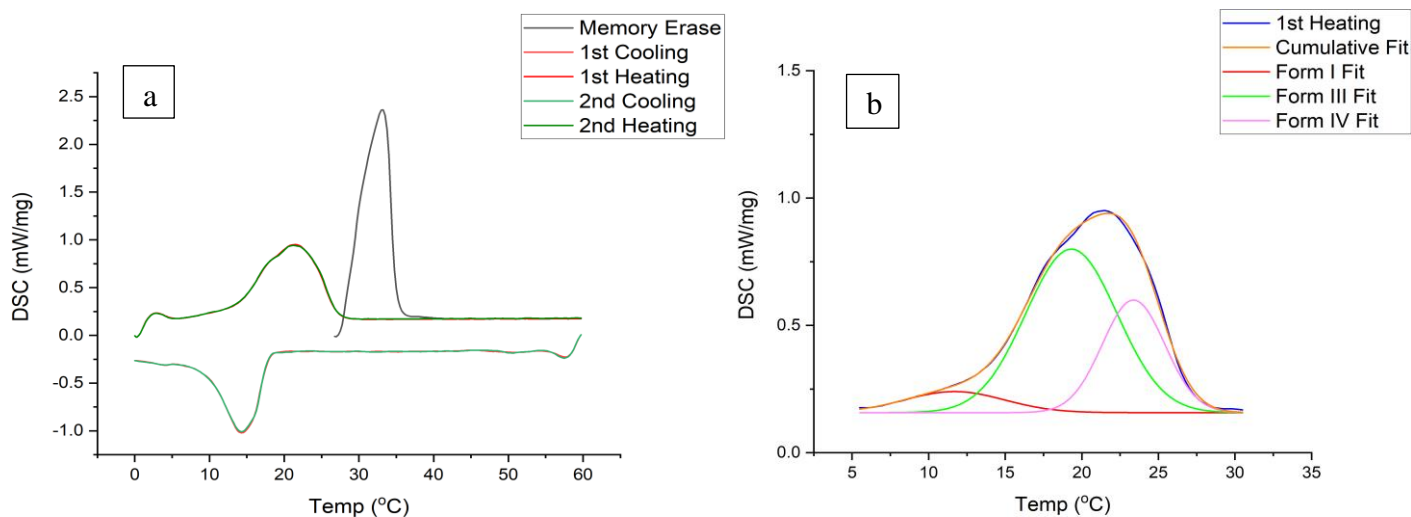


Figure 5: a) DSC curves for Form II with a cooling/heating rate of 5K/min. As before the bigger peak (black) that appears indicates the melting of Form V crystals. The melting steps overlap and cover the expected temperature range of Form II crystals melting. b) Fitted DSC data for the first heating. The red line is close to the melting point of Form I with a peak at 11.6°C while the green one peaks at approximately 19.3°C which is close to the melting threshold of Form III. The purple one is placed at 23.3°C which is between the end of Form III melting range (19.5 – 21.5°C) and the beginning of Form IV’s range (25.5 – 28°C). The orange line is the cumulative fit.

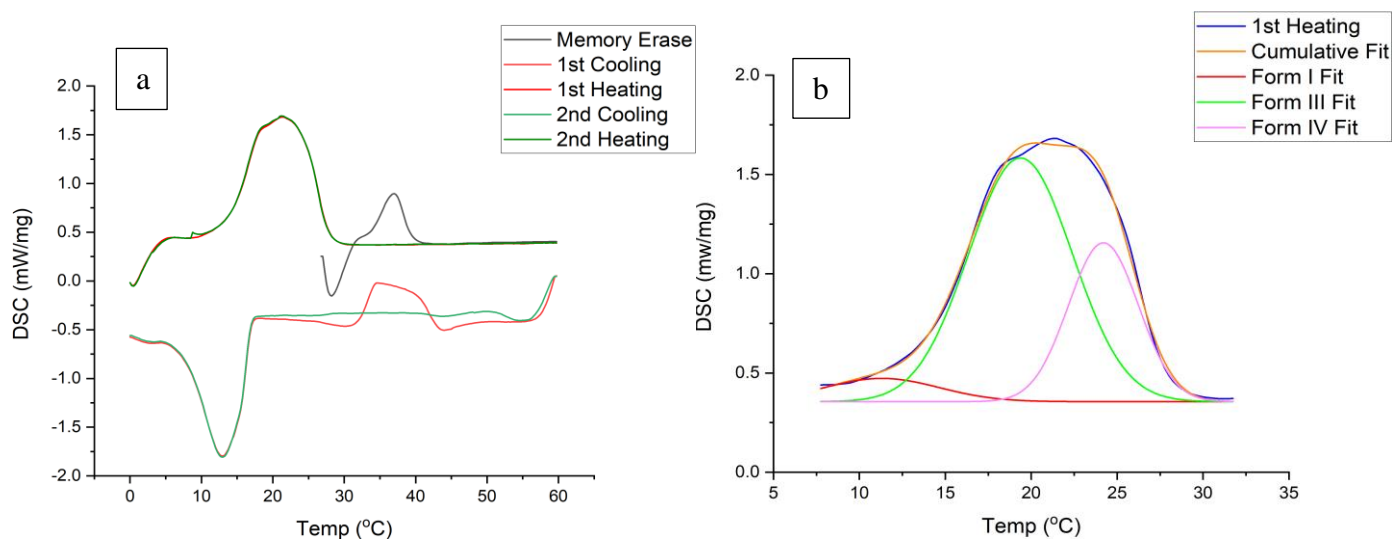


Figure 6: a) DSC curves for Form II with a cooling/heating rate of 10K/min. The curve that corresponds to the memory erase is lower to intensity than the previous ones. Also, we notice a different behaviour for the 1st cooling after the memory erase. It seems due to the faster heat flow rate that some crystals have not completely melted, thus the endothermic indication while the sample is under cooling conditions. b) Fitted DSC data for the first heating. As for the 5K/min same indications can be observed here as well. The fitting shows signs of Form I, III and IV with the peaks placed at approximately 11.3, 19.3 and 24.2°C respectively.

For 5K/min and 10K/min rates the fitting revealed the existence of Form I, III and IV crystals and the lack of pure Form II crystals. Comparing the fitted peaks with the values from Table 1 supports the notion that slower cooling rates help with the isolation of Form II crystals while higher rates do not provide the sample enough time to crystallize in the desired Form.

DSC curves for Form III can be seen in figures 7-9. The protocol suggests a cooling rate of 2K/min until 14°C and afterwards an isothermal rest for 1 hour. Measurements were also made with heating/cooling rates of 5K/min and 10K/min. Once again, one common feature on all our curves is the presence of a peak associated with the memory erase placed close to 32°C. In Figure 7 the curves for 2K/min are illustrated. After fitting the heating parts with a Gaussian function, there are indications that Form III and IV crystals co-exist with crystals of Form II. Figure 8 shows the DSC measurements for 5K/min and Figure 9 for 10K/min.

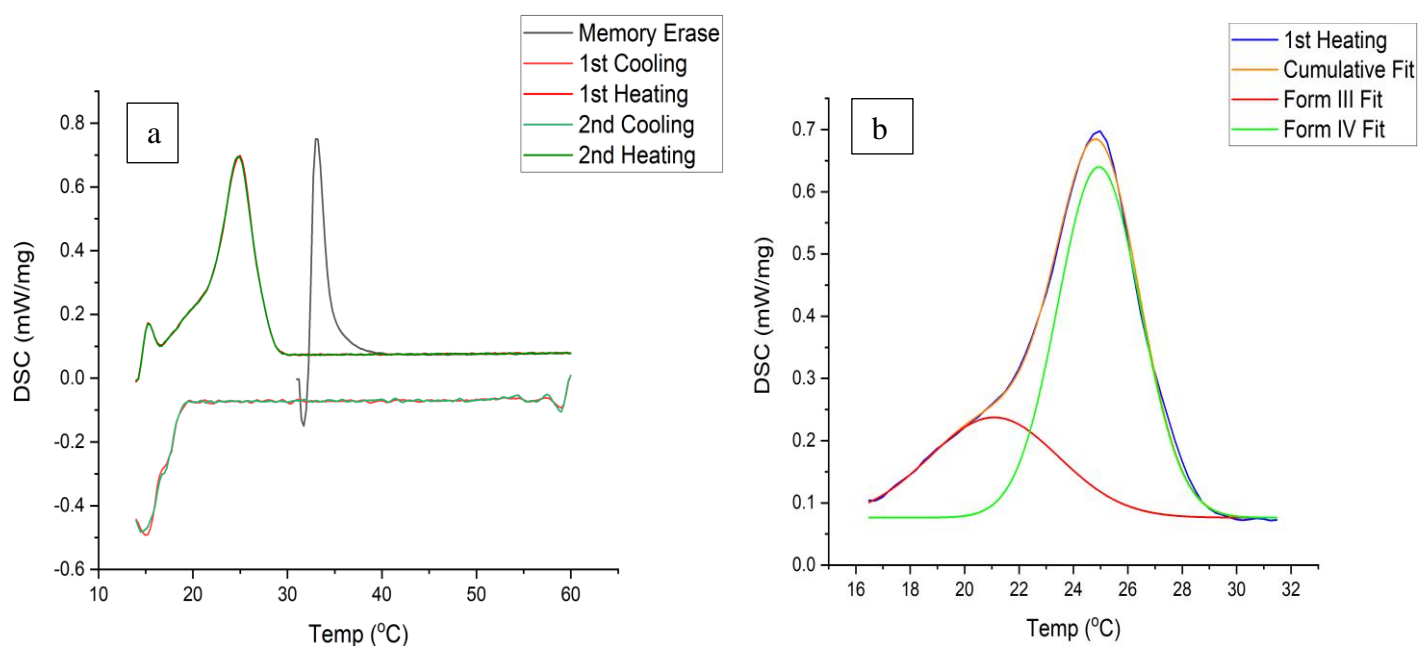


Figure 7: a) DSC curves for Form III with a cooling/heating rate of 2K/min. The black line corresponds to the memory erase heating that precludes all our measurements. The curves overlap each other representing the reproducibility of our measurements. The melting ranges indicate the melting of Form III crystals. b) Fitted DSC data for the first heating. Fitting suggests the creation of Form IV crystals alongside Form III crystals. The red curve peaks at 21°C and supports the creation of Form III crystals. The green curve peaks at ~25°C which is close to the melting point of Form IV crystals.

Although the melting range during the heating parts covers the expected area for Form III, fitting indicates the presence of Form IV crystals. Wille and Lutton place the peak melting point for Form III at 25.5°C while Bresson places the start of the melting range for Form IV at the same temperature.

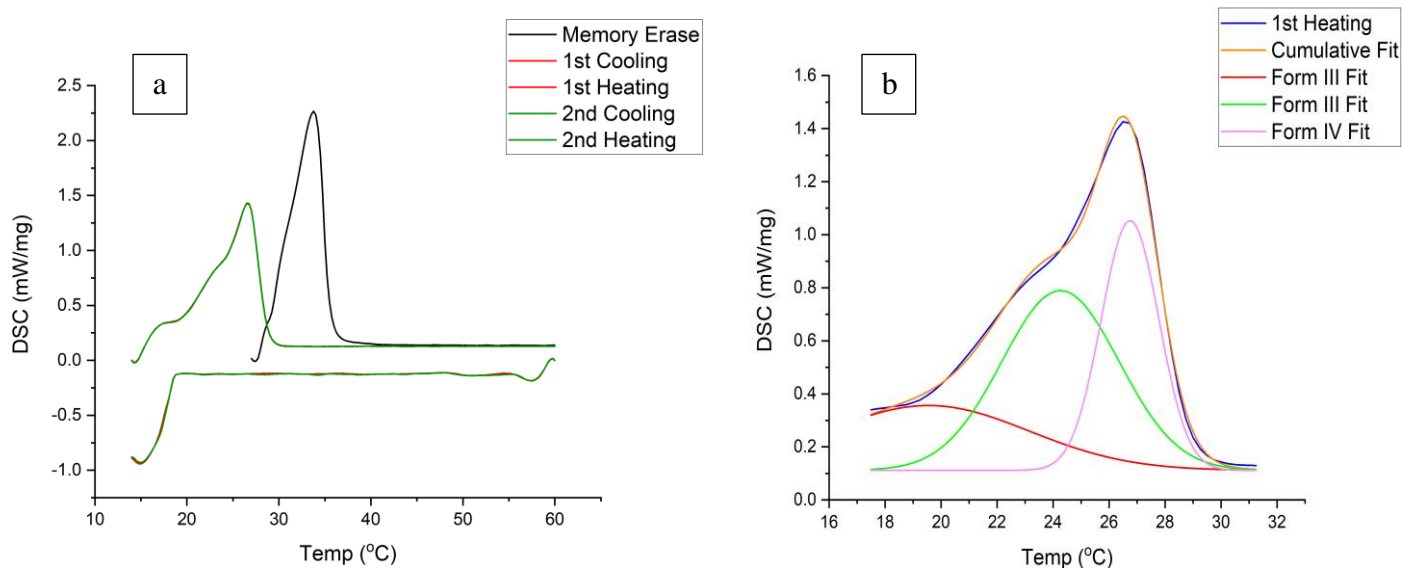


Figure 8: a) DSC curves for Form III with a cooling/heating rate of 5K/min. The black line corresponds to the memory erase heating. The curves overlap each other representing the reproducibility of our measurements. The melting ranges indicate the melting of Form III crystals. b) Fitted DSC data for the first heating. Fitting suggests the creation of Form IV crystals alongside Form III crystals. The red curve peaks at 19.5°C and supports the creation of Form III crystals. The green curve peaks at 24.2°C which is between the two melting ranges of Form III and Form IV. The purple curve peaks at 26.7°C which places it in Form IV’s melting range. The orange curve is the cumulative fit.

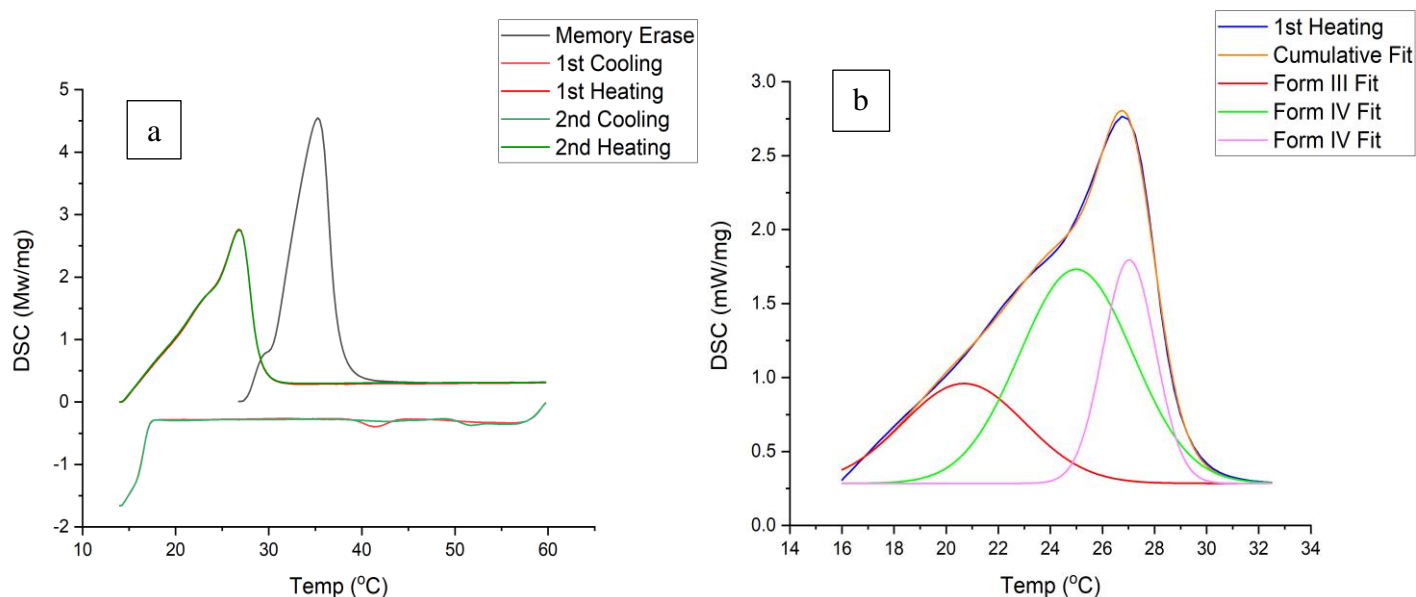


Figure 9: a) DSC curves for Form III with a cooling/heating rate of 10K/min. The black line corresponds to the memory erase heating that precludes all our measurements. The curves overlap each other representing the reproducibility of our measurements. The melting ranges indicate the melting of Form III crystals. b) Fitted DSC data for the first heating. Fitting suggests the creation of Form IV crystals alongside Form III crystals. The red curve peaks at 20.6°C and supports the creation of Form III crystals. The green curve peaks at 25°C which is close to the melting range of Form IV crystals. The purple curve peaks at 27°C which places it in the melting range of Form IV. The orange curve is the cumulative fit.

DSC curves for Form IV can be seen in figures 10 and 11. The protocol suggests a cooling rate of 10K/min until 22°C and afterwards an isothermal rest for 2 hours. An extra measurement with a heating/cooling rate of 5K/min was also executed. In Figure 10 the curves for 5K/min are illustrated and in Figure 11 the one for 10K/min. The melting range corresponds to the melting of Form IV crystals in both cases.

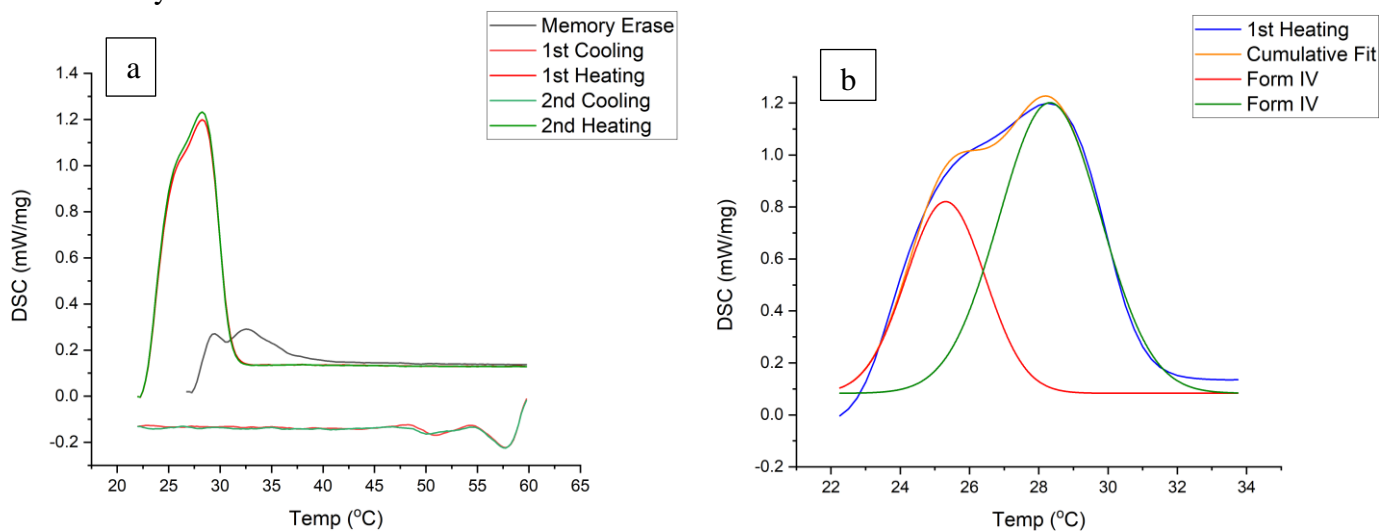


Figure 10: a) DSC curves for Form IV with a cooling/heating rate of 5K/min. The black line corresponds to the memory erase heating. During the heating and cooling the curves mostly overlap each other representing the reproducibility of our measurements. The melting ranges indicate the melting of Form IV crystals. b) Fitted DSC data for the first heating. Fitting suggests the creation of Form IV crystals. The red curve peaks at 25.3°C and supports the creation of Form IV crystals while the green curve peaks at 28.3°C which is the end point of the melting range for Form IV crystals. The orange curve is the cumulative fit.

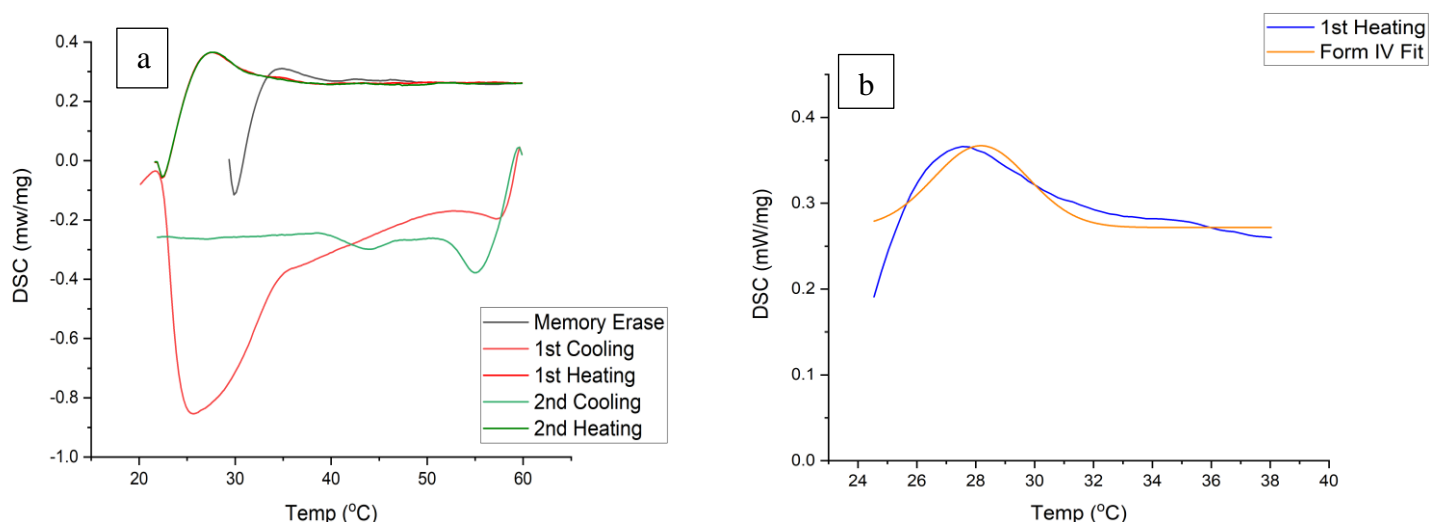


Figure 11: a) DSC curves for Form IV with a cooling/heating rate of 10K/min. The black line corresponds to the memory erase heating. The curves overlap each other during the heating parts. During the cooling parts two completely curves are recorded. This suggests two different crystallization processes. b) Fitted DSC data for the first heating. The orange curve is a fit with a peak at ~28.2°C. The fitting in this case is clearly not close to the real data. This can be caused by the fast heating rate that is used and the buoyance that follows it. It can also suggest that although some crystals were created there was not enough time for the whole sample to crystallize in the desired or a different Form.

4.2 SAXS data

For the X-ray measurements, the SAXS data confirms the crystallization processes and again the reproducibility of the results. X-ray measurements have been conducted for the whole duration of one cycle meaning that after the 10 minutes have passed in which our sample has been kept at 60°C, so no crystal memory effects occur, the sample has been cooled by the specified rate and kept for the specified duration (Figure 1). For example, for Form II the sample has been brought to 0°C with a rate of 2 K/min and kept there for one hour. After that it was heated by 2 K/min until the 60°C mark. Acquisition time was one minute.

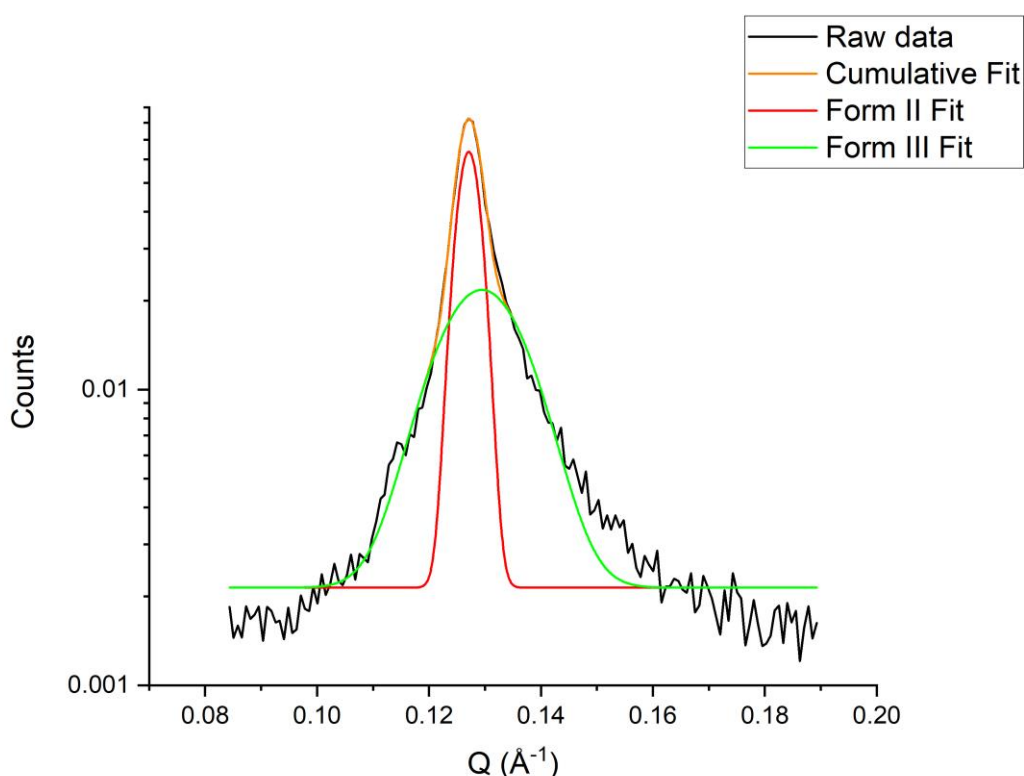


Figure 12: SAXS data for Form II with a cooling rate of 2K/min acquired at the end of the one-hour isothermal rest. The fitting suggests two peaks one at 49.4 Å (red) and the other one at 48.1 Å (green). This indicates the creation of Form II crystals alongside Form III crystals.

Figure 12 illustrates the SAXS data acquired for Form II with a cooling rate of 2K/min. The values on the x-axis are on the q-space. Using Eq. 3 we can reverse this and find the spacings in real space. According to Bresson the long spacing for form II is 49.3 Å and for Form III, which has two long spacings, at 48.5 and 45 Å. Our fitting suggests two peaks at 49.4 and 48.1 Å. This indicates the creation of Form II crystals as well as the presence of Form III crystals. The fitting of the DSC curves also suggested the creation of other forms alongside Form II.

In Figure 13 the SAXS measurements for Form II with a cooling rate of 5K/min is depicted. Fitting indicates three peaks; The first one is situated at 50.9 Å, the second one at 48.1 Å and the third at 44.4 Å. These values are far from the expected one which is 49.3 Å. The values are closer to those of Form I, III and IV something that was also indicated by the DSC measurements and fitting.

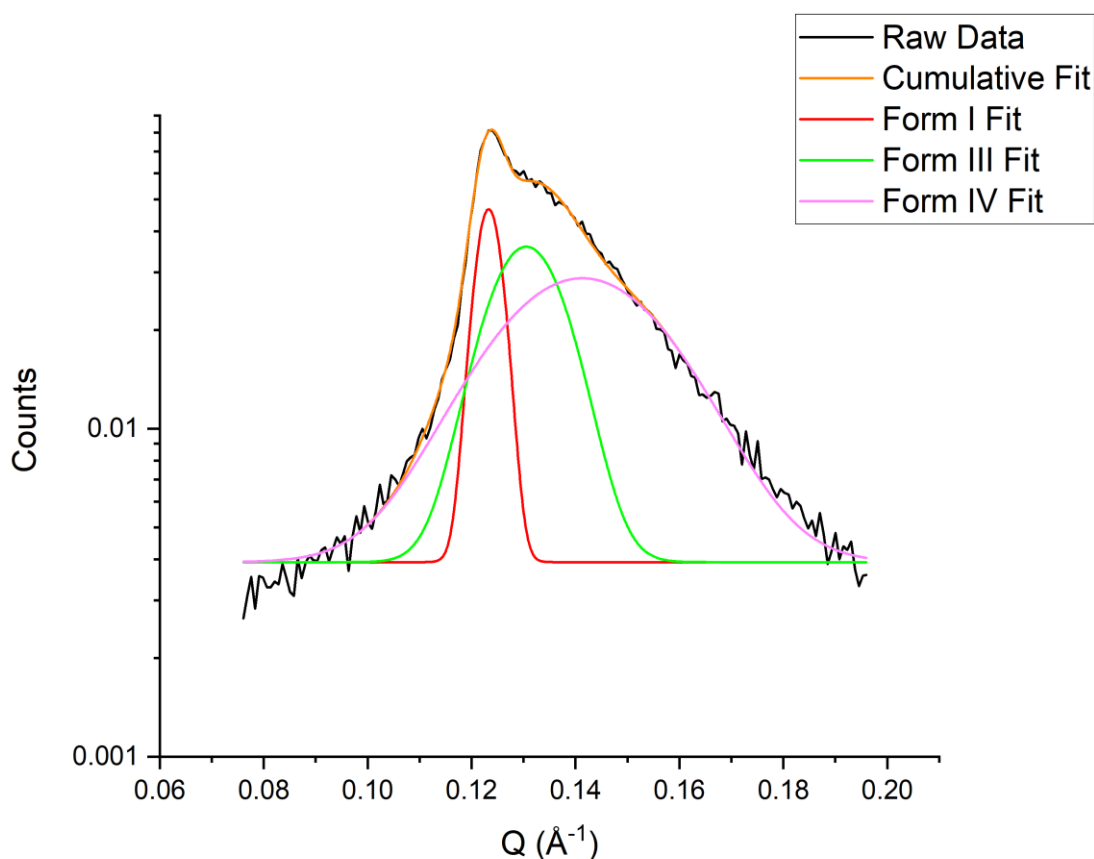


Figure 13: SAXS data for Form II with a cooling rate of 5K/min acquired at the end of the one-hour isothermal rest. The fitting suggests three peaks: 50.9 Å (red), 48.1 Å (green) and 44.4 Å (purple). This indicates the creation of Form I, III and IV crystals.

Figure 14 shows the SAXS measurements for Form II with 10K/min. Fitting suggests three peaks: 51.5, 47.9 and 45.1 Å. The first peak is far from Form I (50.8 Å) which was expected to be created based on the previous measurement. It also falls far from all the recorded values that Bresson presents. The two remaining peaks are closer to values suggesting the creation of Form III crystals. This was also suggested by the fitting of the DSC curves.

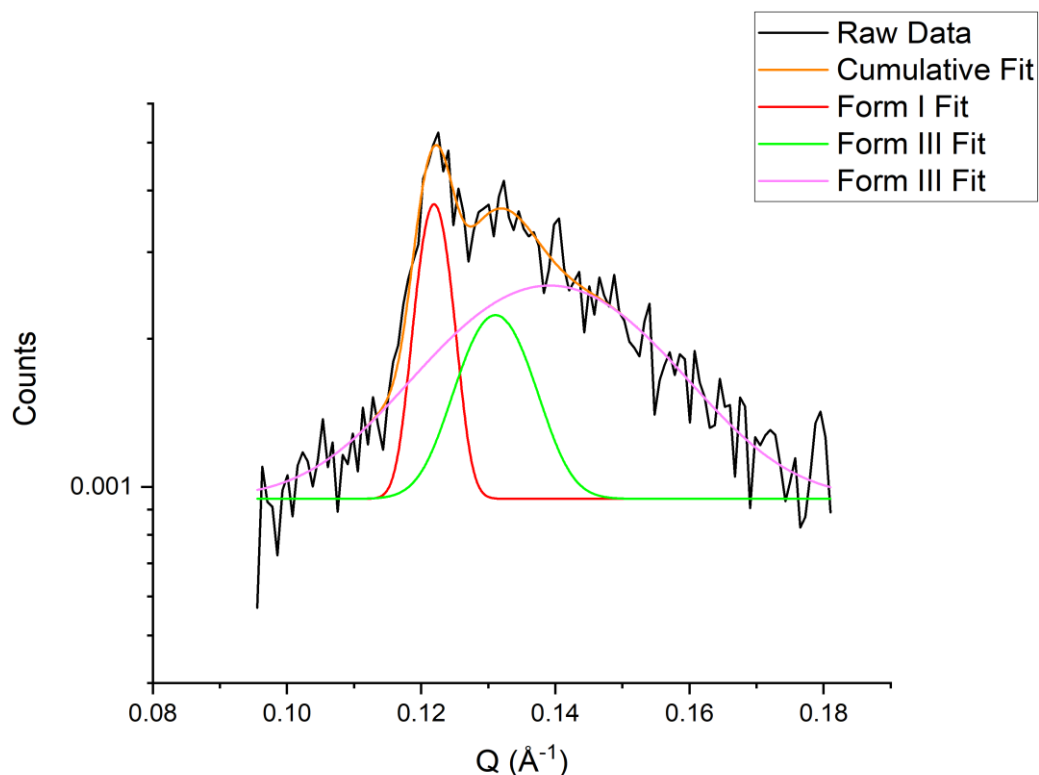


Figure 14: SAXS data for Form II with a cooling rate of 10K/min. The fitting suggests three peaks: 51.5 Å (red), 47.9 Å (green) and 45.1 Å (purple). This indicates the creation of Form I, III and IV crystals.

Following are the measurements for Form III. Form III is the only Form with two values for its long spacings. Figure 15 shows the SAXS measurement for Form III with 2K/min cooling rate. The first peak is at 48.7 Å putting it very close to the expected value of 48.5 Å. The other peak is at 46.2 Å which places it far from the expected value of 45 Å.

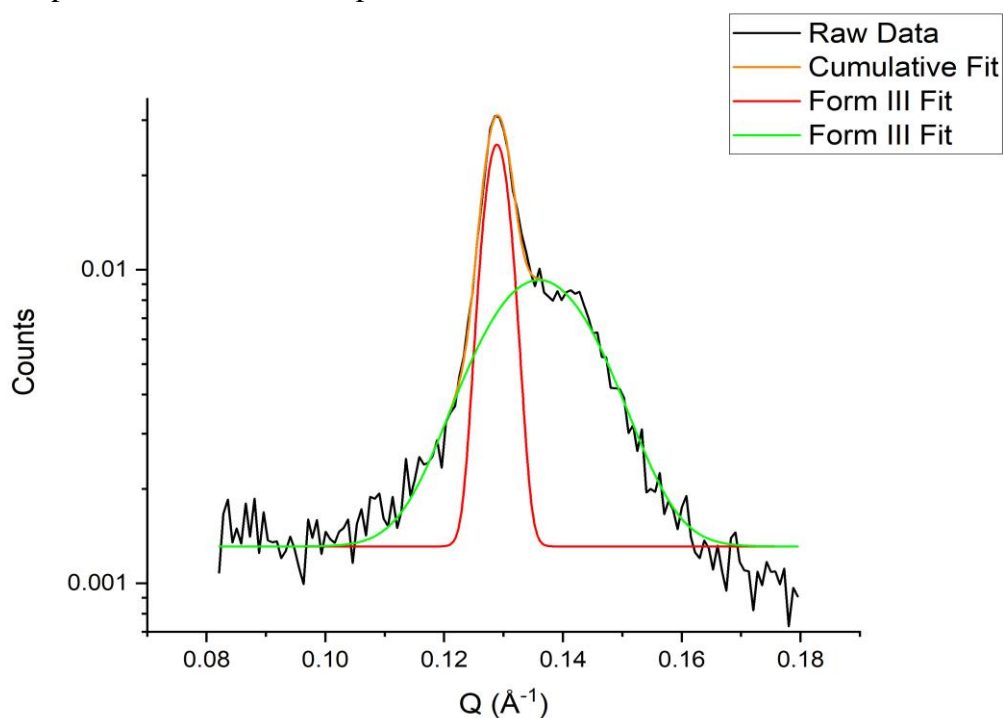


Figure 15: SAXS measurements for Form III with a cooling rate of 2K/min. The fitting suggests two peaks with values of 48.7 and 46.2 Å.

Form III with 5K/min is presented in Figure 16. Two peaks have been fitted with spacings of 48.7 and 46.3 Å, very similar to the previous values. Figure 17 shows the SAXS data for 10K/min which again places the peaks at 48.7 and 46.4 Å. Form III seems to be affected less by the heating rate compared to Form II.

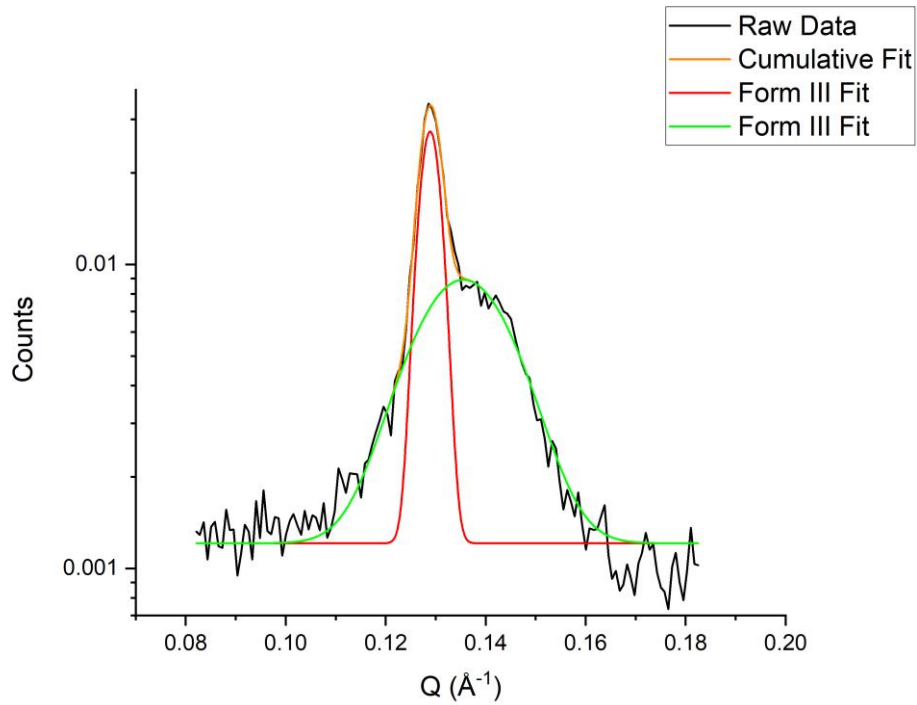


Figure 16: SAXS data for Form III at the end of the cooling process with a cooling rate of 5K/min. Fitting suggests two peaks with values of 48.7 and 46.3 Å.

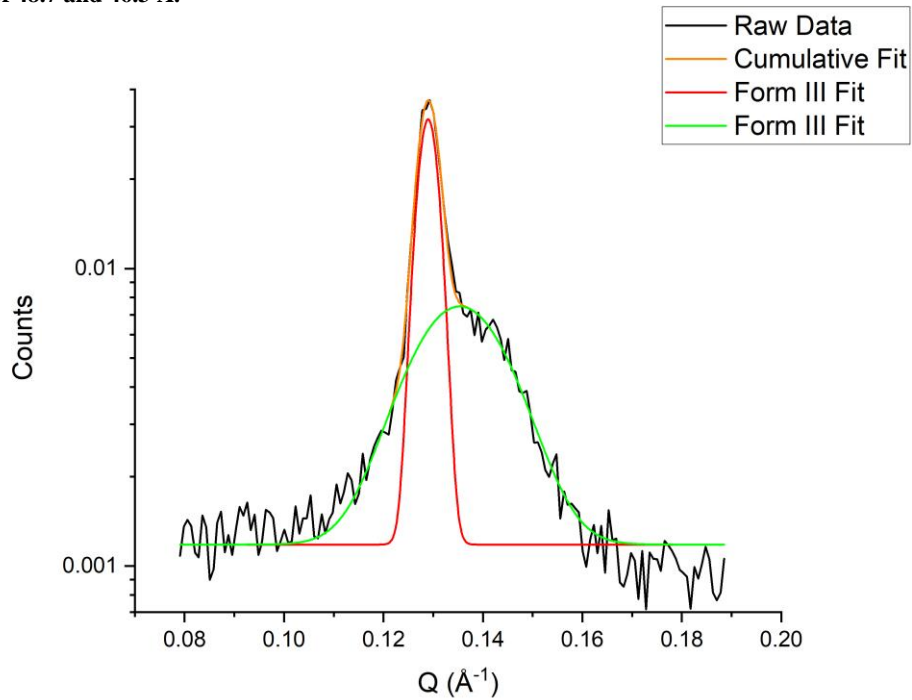


Figure 17: SAXS data for Form III with 10K/min. Two peaks have been fitted at 48.7 and 46.4 Å.

The last of the SAXS measurements concern Form IV. Two cooling/heating rates have been used for these measurements unlike the other two forms. Figure 18 shows the SAXS data for 5K/min and Figure 19 for 10K/min. In both cases the spacing suggested by the fitting is 45 Å. The intensity for both measurements is low compared to the previous Forms. This can be attributed to insufficient time spent at isothermal rest even though the sample was held at 22°C for 2 hours.

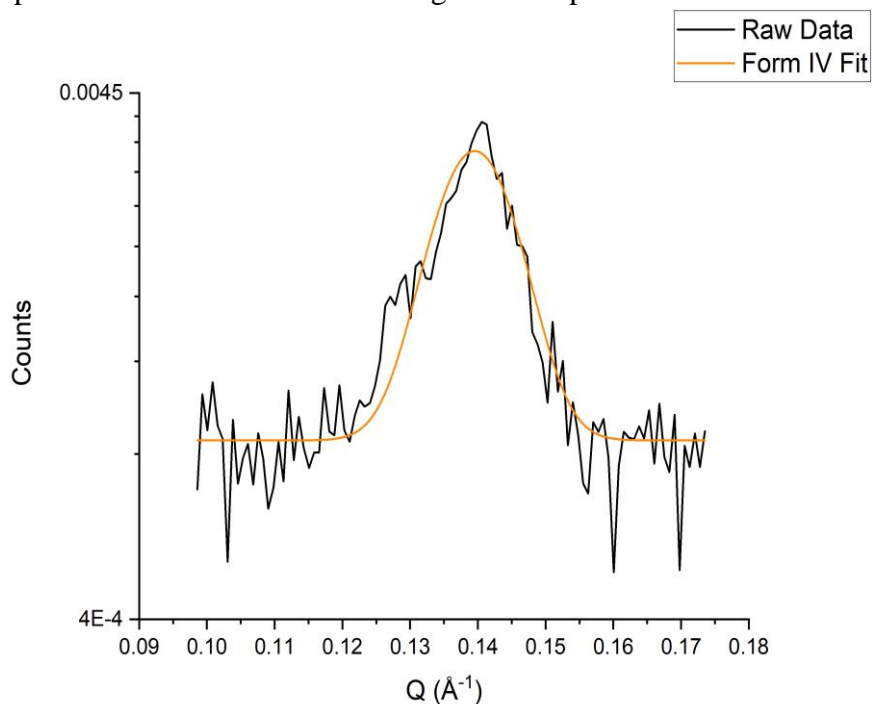


Figure 19: SAXS data at the end of the 2-hour isothermal rest with a heat flow rate of 5K/min. The fitting suggests one peak with a value of 45 Å.

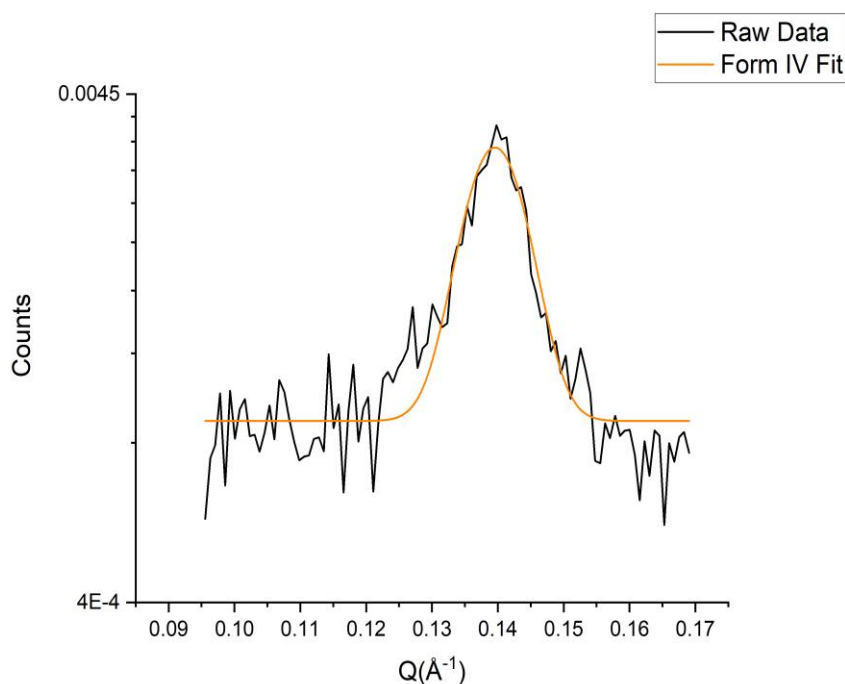


Figure 20: SAXS data for Form IV with a heat flow rate of 10K/min. Fitting suggests one peak with a value of 45 Å.

4.3 WAXS data

The instrument allowed us for simultaneous measurements, meaning that the SAXS and WAXS data have been acquired at the same time. This ensures us that we recorded all the phenomena that occurred at both short and long spacings and not tempered with the sample by any means (mounting/unmounting for example) between methods.

Figures 21-23 show the measurements for Form II with the three heat flow rates of 2K/min, 5K/min and 10K/min respectively. In all cases similar spacings have been found. Indications for the creation of more Forms than just Form II are present in all cases.

In Figure 21 the WAXS data for 2K/min is presented. The fitting suggests three peaks with centres at 4.23, 4.28 and 4.39 Å. These values suggest the creation of Form III (4.28 Å) and IV (4.39 Å) crystals alongside Form II.

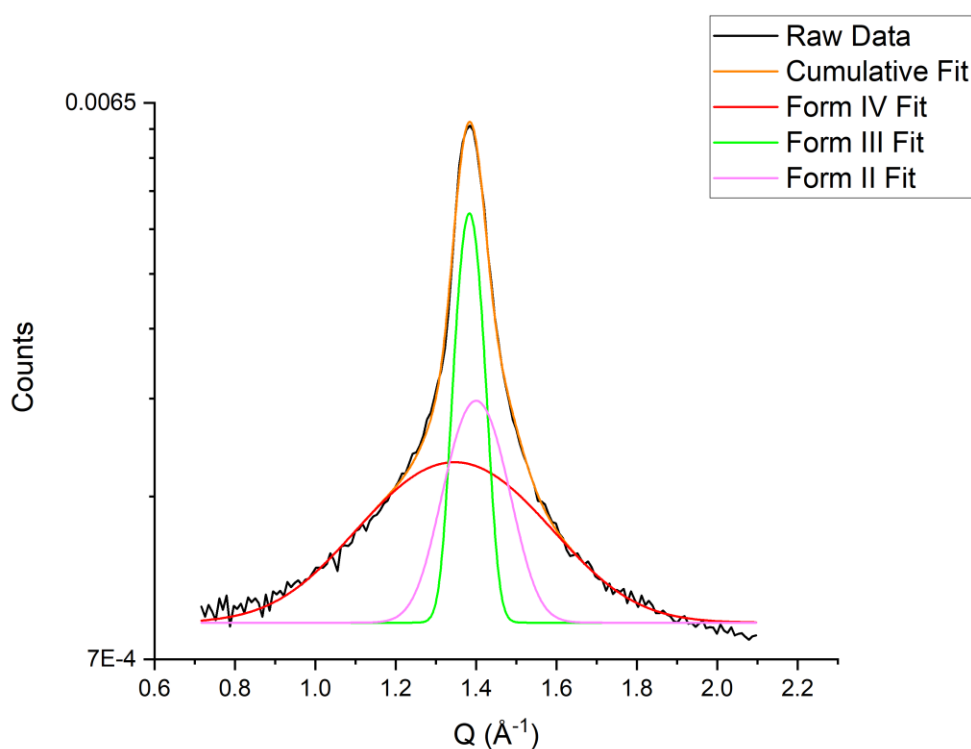


Figure 21: WAXS data for Form II at the end of the one-hour isothermal rest at 0°C and a heat rate flow of 2K/min. The fitting gives us three peaks with centres placed at 4.39 (red), 4.28 (green) and 4.23 (purple) Å. The orange curve is the cumulative fit.

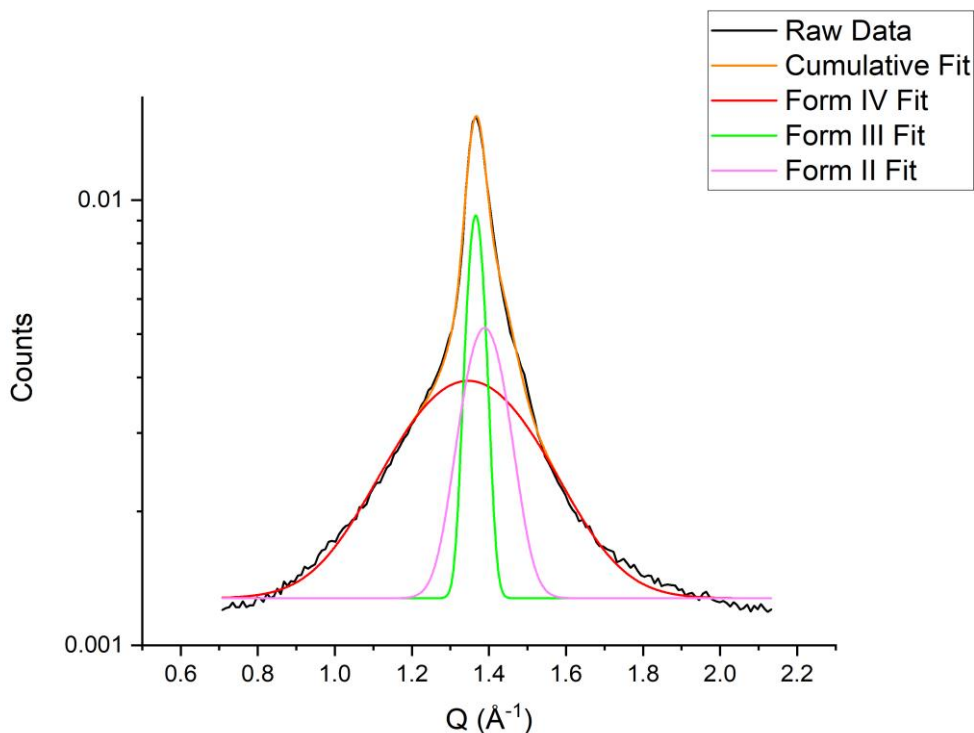


Figure 22: WAXS data for Form II with a heat rate flow of 5K/min. Three peaks with centres at 4.39 (red), 4.33 (green) and 4.26 (purple) Å have been fitted. The orange curve is the cumulative fit.

Figure 22 shows the WAXS data for Form II with a heat flow rate of 5K/min. The three fitted peaks give us short spacings of 4.39, 4.33 and 4.26 Å which correspond to Form IV, III and II respectively. Compared to the results of 2K/min we notice that the value that has changed significantly is the one for Form III at 4.33 Å.

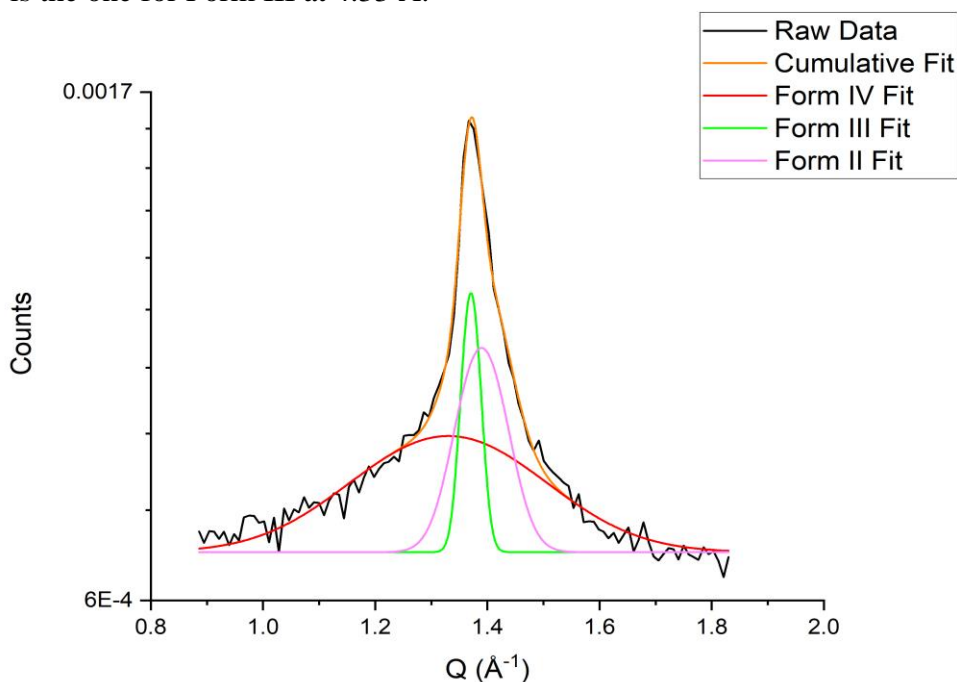


Figure 23: WAXS data for Form II with 10K/min. Three peaks are fitted with centres at 4.44 (red), 4.31 (green) and 4.26 (purple) Å. The orange curve is the cumulative fit.

In Figure 23 the WAXS data for Form II with a heat flow rate of 10K/min is presented. The fitted peaks centre at 4.44, 4.31 and 4.26 Å. Compared to the previous measurement with a heat flow of 5K/min, we notice the elongation of the first spacing (4.44 Å) that is close to one of the Form IV spacings and a slight subtraction of the middle spacing (4.31 Å) that is comparable to Form III.

The WAXS data for Form III with a heat flow rate of 2K/min is in Figure 24. Three peaks are fitted with centres that result in spacings of 4.32, 4.27 and 3.93 Å. Form III according to Bresson exhibits spacings of 4.28 and 3.9 Å. Two of the spacings that we have measured are very close to these values. However, one more spacing is found at 4.32 Å which puts it close to Form IV spacing of 4.38 Å.

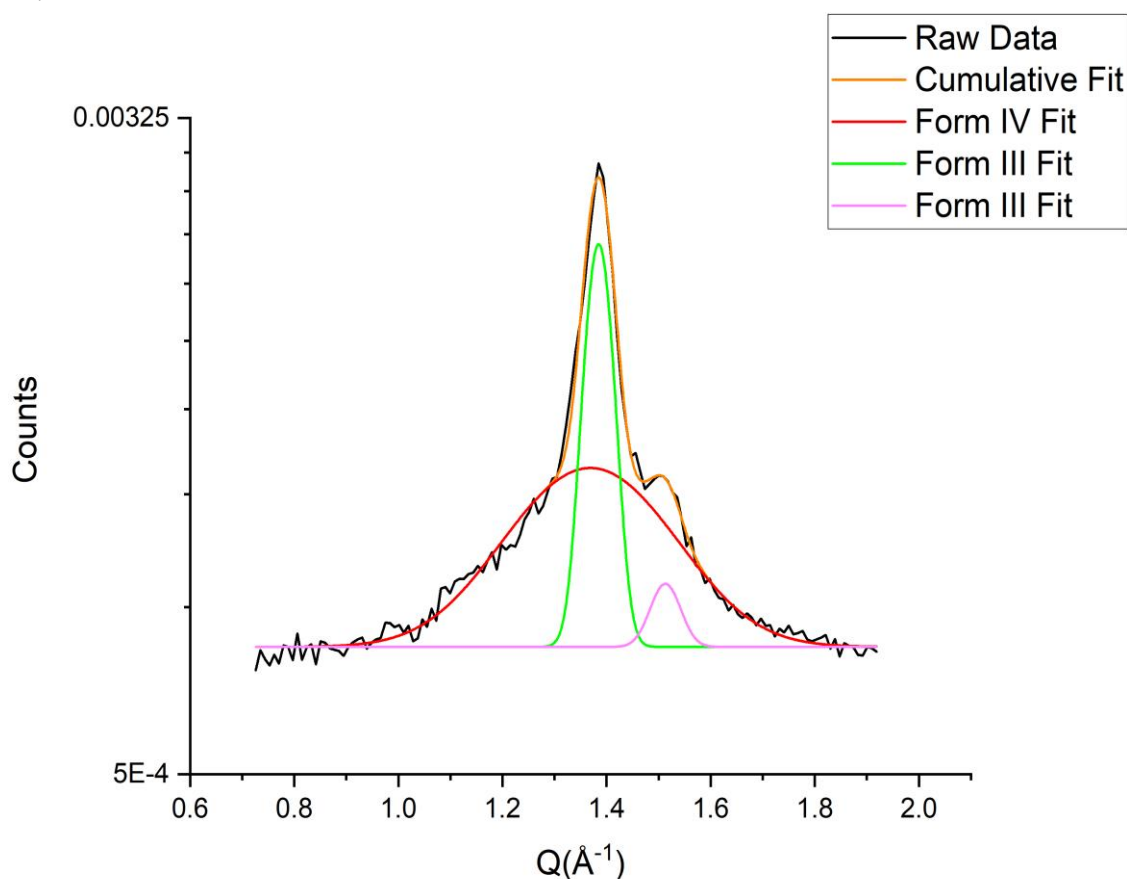


Figure 24: WAXS data for Form III at the end of the one-hour isothermal rest at 14°C with a heat flow rate of 2K/min. Three peaks are fitted with values of 4.32 (red), 4.28 (green) and 3.93 (purple) Å. The orange curve is the cumulative fit.

Figure 25 shows the WAXS data for Form III with 5K/min. The fitting reveals three peaks with values of 4.3, 4.27 and 3.92 Å. Very similar spacings when comparing to the data acquired with 2K/min.

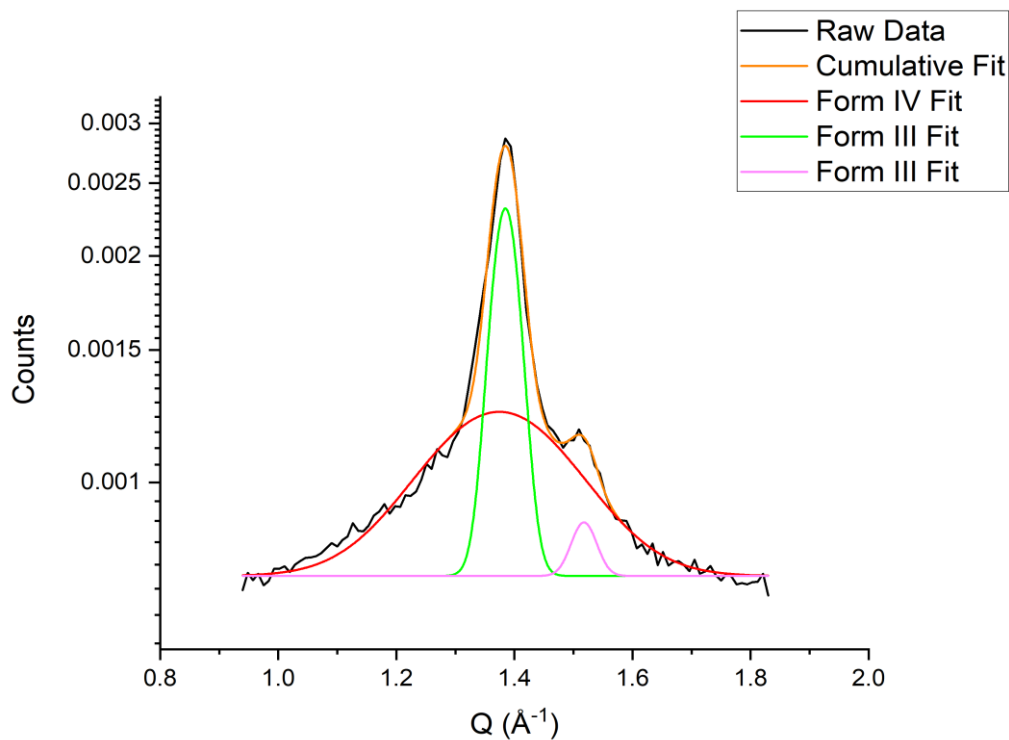


Figure 25: WAXS data of Form III with 5K/min. Three peaks are fitted which represent spacings of 4.3 (red), 4.27 (green) and 3.92 (purple) Å. The orange curve is the cumulative fit.

The last WAXS measurement for Form III is illustrated in Figure 26. A heat flow rate of 10K/min is used and the spacings that are extracted from the fitting are 4.31, 4.27 and 3.92 Å. The spacings are almost identical to the previous ones.

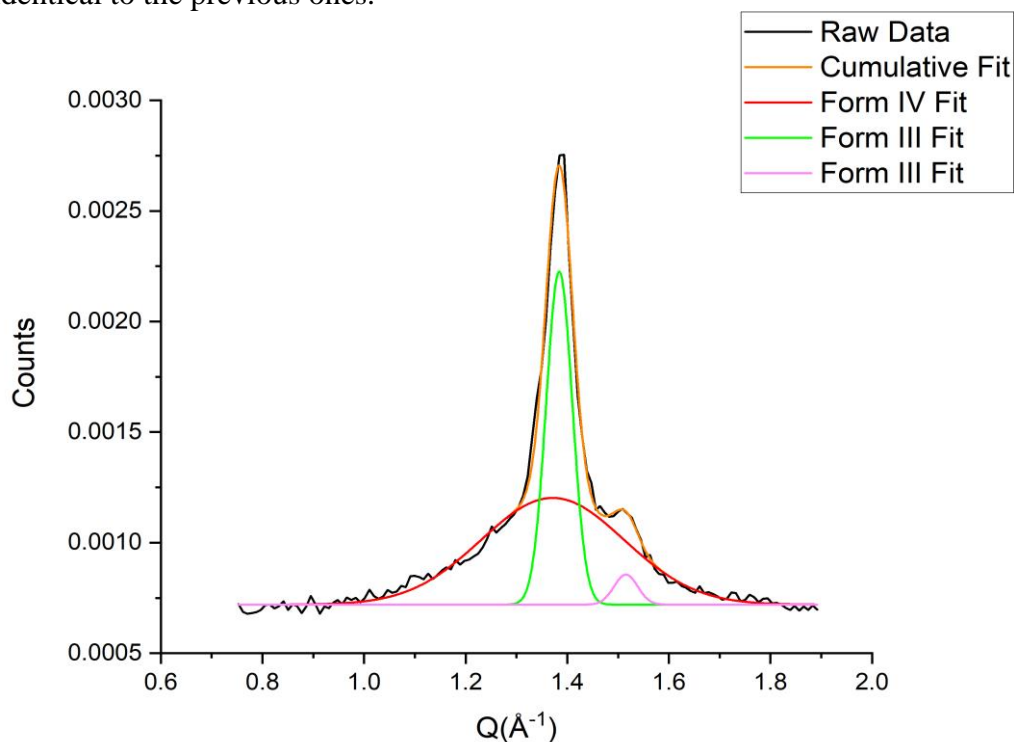


Figure 26: WAXS data for Form III with 10K/min heat flow rate. The fitting suggests three peaks with centres at 4.31 (red), 4.27 (green) and 3.92 (purple) Å. The orange curve represents the cumulative fit.

The results that are presented in Figures 27 and 28 concern Form IV. For 5K/min, Figure 27, the spacings that were extracted have values of 4.59 and 4.41 Å. From these two values only the second one is close to the reported value of 4.38 Å that corresponds to Form IV crystals. The other value is close to that of Form V crystals that have a spacing of 4.6 Å among others. Almost the same values can be observed while the sample is under the 10K/min heat flow rate, Figure 28. The spacings that are observed from the fitting of the WAXS data in Figure 28, have values of 4.56 and 4.4 Å.

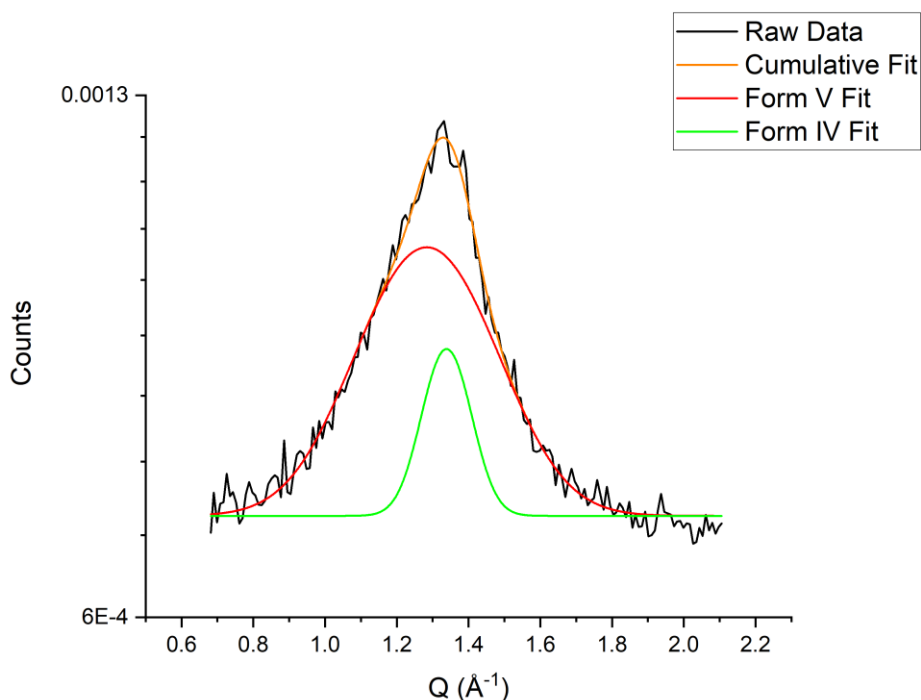


Figure 27: WAXS data for Form IV acquired at the end of the two-hour isothermal rest at 22°C with a heating/cooling rate of 5K/min. The spacings that are indicated by the fitting have values of 4.59 (red) and 4.41 (green) Å. The orange curve is the cumulative fit.

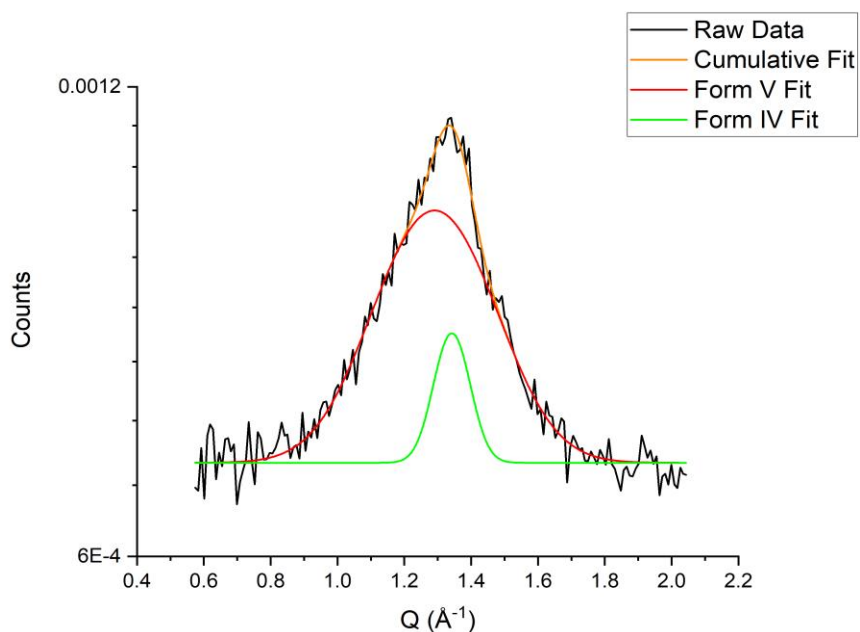


Figure 28: WAXS data for Form IV with 10K/min. The spacings that are extracted have values of 4.56 (red) and 4.4 (green) Å. The orange curve is the cumulative fit.

4.4 Crystallization process

Having an image every minute through the X-ray measurements helps us record key moments for the crystallization process. Starting from Form II at 2K/min we can see that after the initial heating to 60°C and the start of the cooling part it takes approximately 23 minutes for any sign of a crystal to be recorded by our instrument; the temperature at this point is ~17°C. After that two peaks appear one larger (~49.4 Å) and one smaller (~54.4 Å). After 5 minutes, the smaller peak starts to move to the right (towards smaller spacings) and lose intensity while the larger one stabilizes and gains intensity (temperature at ~6°C). Reaching 0°C only one peak is visible. For 5K/min the first sign of crystallization is after reaching ~18°C. One peak starts to form, which as the temperature decreases and reaches 0°C moves to the right and loses intensity. A second peak starts to form after the sample has been cooling for approximately 15 minutes. Finally, one peak remains after the sample has been cooling for a total of 22 minutes. Last is the 10K/min measurement. At ~7°C signs of crystallization can be observed. Reaching 0°C the first peak (~54.6 Å) can be clearly seen. Three minutes after this point the peak loses intensity and moves to the right while a second peak starts forming. One peak remains visible after cooling for ~20 minutes.

For Form III and a heat flow rate of 2K/min the following can be said: After the cooling starts from 60°C it takes approximately 22 minutes for any sign of crystallization to be detected by our instrument. One peak starts forming when the temperature reaches ~15°C (spacing of 49.3 Å). Another peak starts forming soon after (spacing of 54.3 Å) and reaches max intensity. After approximately 30 minutes of cooling, the peak loses intensity and completely disappears. As previously mentioned, Form III has two long spacings. The expected second peak starts to form after 50 minutes of cooling. The measurement with 5K/min shows faster crystallization, with signs of a crystal structure showing after 9 minutes of cooling from 60 to 14°C. The first peak starts forming (~49.3 Å) and a 2nd peak follows soon after (~54.5 Å). 15 minutes have passed since the cooling started and the 2nd peak starts to lose intensity until it is completely gone 3 minutes after. The expected 2nd peak starts forming 35 minutes into the cooling process and can be clearly observed after 50 minutes. At the end of the one-hour isothermal at 14°C both peaks are formed. Lastly, the measurement for 10K/min shows us even faster signs of crystallization after 8 minutes of cooling. The first peak forms (~49.5 Å) the next minute and a 2nd peak starts forming (~54.2 Å) soon after. 17 minutes of cooling pass for the 2nd peak to disappear and only the first peak remains. The expected 2nd peak starts to take shape after 1 hour of cooling (~58 minutes of isothermal rest) and gains intensity.

Form IV has been recorded with two rates: 5K/min and 10K/min. For 5K/min, 21 minutes of cooling pass for the first sign of crystallization to be observed. One peak is formed ($\sim 49.7 \text{ \AA}$) 10 minutes after that. A second peak starts forming ($\sim 44.5 \text{ \AA}$). 56 minutes of cooling and the 1st peak starts to lose intensity and moves right. After two hours of cooling the 1st peak almost disappears. The last measurement takes place after 128 minutes with the 1st peak showing slight signs of still existing. With a cooling rate of 10K/min approximately the same time is needed for a peak to start forming. 42 minutes of cooling have passed, and a peak has formed ($\sim 49.7 \text{ \AA}$). It takes approximately 50 minutes for a 2nd peak to form ($\sim 44.5 \text{ \AA}$). 1st peak disappears after 125 minutes of cooling.

5. Discussion and Conclusion

For all our measurements, we have indications proving the difficulty of the isolation of the three crystal Forms. Starting from the fitted DSC measurements we can observe hints that more Forms are present than the expected one. With the help of the X-ray scattering techniques, we have further indications supporting this.

For Form II and 2 K/min the fitting of the DSC data suggests Form II, III and IV. The WAXS measurements indicate the existence of Form II, III and IV and the SAXS data shows Form II and III. For 5K/min the DSC measurement indicate Form I, III and IV. The WAXS measurements indicate Form IV and a spacing that is between Form III and II. SAXS data shows spacings of Form I, III and IV. The last DSC measurement with a heating/cooling rate of 10K/min, for Form II, shows signs of Form I, III and IV. WAXS data indicate the creation of Form IV and gives rise to a spacing that is between Form II and III. SAXS data indicate the creation of Form I and III. Raising the heat flow rate seems to hinder the creation of Form II crystals. Going back to Bresson, the suggestion for Form I creation is a fast cooling rate (quenching) until -10°C and a short isothermal rest for 10 minutes. Form IV creation needs a cooling rate of 10K/min to form. Keeping these in mind, we can assume that raising the cooling rate supports the creation of Form I crystals in combination with the 0°C temperature. We notice that the intermediate rate of 5K/min gives us long spacings of Form I, III and IV but a short spacing that is between Form II and III, and another one close to IV. Raising the rate to 10K/min seems to promote Form III crystals in the long spacing and affect the short spacing that is close to Form IV. In conclusion, a slow heat flow rate and a slight increase in the duration of the isothermal rest should promote the creation of pure Form II crystals.

The fitting of the DSC curves for Form III at 2K/min suggests the co-existence of Form III and IV. WAXS data indicate the creation of the same Forms. SAXS data shows clear signs of one of the two spacings that are related to Form III and places the other one far from the reported value. The same observations can be made for 5K/min as well as 10K/min. Form III seems to be less affected compared to Form II by the heat flow rate. DSC data indicate the existence of Form IV alongside III. This is also the case for the SAXS and WAXS data. Since Form III has two spacings in the SAXS region, where one of them is formed quicker than the other, an increase in the time that the sample spends in isothermal rest is suggested to give enough time for the second spacing to be developed.

Form IV seems to be the one that is easier to isolate. DSC data for both rates indicate the creation of Form IV crystals. This is further supported by the SAXS data. However, WAXS data indicates a spacing close to that of Form V. Bresson suggests quenching for the creation of Form V crystals alongside a long period of isothermal rest (7 days). For the X-ray measurements concerning Form IV an increase in the isothermal rest duration was also executed. Our signal for Form IV during the X-ray measurements remained low. The expected peaks started forming very close to the end of the two-hour isothermal rest (no increase of the isothermal duration for our measurements). An increase in the isothermal rest period is suggested. The cooling rate of 10K/min seems to provide the desired results.

All the data acquired by the X-ray scattering are provided in the following tables for clarity.

	2K/min	5K/min	10K/min
Form II	49.4 Å	50.9 Å	51.5 Å
(Expected value 49.3 Å)	48.1 Å	48.1 Å	47.9 Å
		44.4 Å	45.1 Å
Form III	48.7 Å	48.7 Å	48.7 Å
(48.5 and 45 Å)	46.2 Å	46.3 Å	46.4 Å
Form IV (44.8 Å)		45 Å	45 Å

Table 2: SAXS results of all three Forms. Forms, spacings and heating rates are presented. The expected value is the value that Bresson indicates for each Form using the protocol of Figure 1.

	2K/min	5K/min	10K/min
Form II	4.39 Å	4.39 Å	4.44 Å
(Exp. Value 4.24 Å)	4.28 Å	4.33 Å	4.31 Å
	4.23 Å	4.26 Å	4.26 Å
Form III	3.93 Å	3.92 Å	3.92 Å
(4.28 and 3.9 Å)	4.27 Å	4.27 Å	4.27 Å
	4.32 Å	4.30 Å	4.31 Å
Form IV		4.41 Å	4.40 Å
(4.38 and 4.19 Å)		4.59 Å	4.56 Å

Table 3: WAXS results for all three Forms. Forms, spacings and heating rates are presented. The expected value corresponds to the value reported by Bresson following the protocol of Figure 1.

PERSPECTIVES

The isolation of the desired Forms proved hard. The in-situ X-ray measurements provided an in-depth view of the crystallization process which can be used to further study cocoa butter. It would prove beneficial to check if after the creation of one Form further cooling would force the crystals to re-arrange and provide a different, isolated Form, or the memory effect and the fact that the sample has already been crystallized to a specific Form hinder this. The answer to this might benefit the research for stabilizing and extending the life of Form V crystals which is important to the food industry. Also, the rest of the Forms might prove useful for other industries since cocoa butter is a natural and safe to use product.

Cocoa butter can be structured with different percentages of specific TAGs, understanding the nucleation process might help us determine if we should focus more on the building blocks, that are the TAGs, or the final product which is the cocoa butter. This can be the next focus point for dedicated research.

Nevertheless, the research conducted has produced enough data for understanding the difficulty of isolating the Forms, provided insight on the importance of the cooling rate and resulted in a map for the crystallization process.

BIBLIOGRAPHY

1. Bayés-García, Calvet, T., Àngel Cuevas-Diarte, M., Ueno, S., & Sato, K. (2013). *In situ observation of transformation pathways of polymorphic forms of 1,3-dipalmitoyl-2-oleoyl glycerol (POP) examined with synchrotron radiation X-ray diffraction and DSC.* *CrystEngComm*, 15(2), 303–314.
2. Beckett, S. T. (2000). *Science of chocolate.* Royal Society of Chemistry.
3. Dewettinck, Foubert, I., Basiura, M., & Goderis, B. (2004). *Phase Behavior of Cocoa Butter in a Two-Step Isothermal Crystallization.* *Crystal Growth & Design*, 4(6), 1295–1302.
4. Garti, & Widlak, N. R. (2012). *Phase Behavior of Saturated Triacylglycerides - Influence of Symmetry and Chain Length Mismatch.* In *Cocoa Butter and Related Compounds* (pp. 1–1). AOCS Press.
5. Declerck, Nelis, V., Danthine, S., Dewettinck, K., & Van der Meeren, P. (2021). *Characterisation of fat crystal polymorphism in cocoa butter by time-domain nmr and dsc deconvolution.* *Foods*, 10(3), 520
6. Chaiseri, & Dimick, P. (1995). *Dynamic crystallization of cocoa butter. I. Characterization of simple lipids in rapid- and slow-nucleating cocoa butters and their seed crystals.* *Journal of the American Oil Chemists' Society*, 72(12), 1491–1496.
7. Fessas, Signorelli, M., & Schiraldi, A. (2005). *Polymorphous transitions in cocoa butter: A quantitative DSC study.* *Journal of Thermal Analysis and Calorimetry*, 82(3), 691–702.
8. Kinta, & Hartel, R. W. (2010). *Bloom Formation on Poorly-Tempered Chocolate and Effects of Seed Addition.* *Journal of the American Oil Chemists' Society*, 87(1), 19–27.
9. Loisel, Keller, G., Lecq, G., Bourgaux, C., & Ollivon, M. (1998). *Phase transitions and polymorphism of cocoa butter.* *Journal of the American Oil Chemists' Society*, 75(4), 425–439.
10. Lovegren, Gray, M. S., & Feuge, R. O. (1976). *Effect of liquid fat on melting point and polymorphic behavior of cocoa butter and a cocoa butter fraction.* *Journal of the American Oil Chemists' Society*, 53(3), 108–112.
11. van Langevelde, van Malssen, K., Peschar, R., & Schenk, H. (2001). *Effect of temperature on recrystallization behavior of cocoa butter.* *Journal of the American Oil Chemists' Society*, 78(9), 919–925.

12. Malssen, Langevelde, A. van, Peschar, R., & Schenk, H. (1999). Phase behavior and extended phase scheme of static cocoa butter investigated with real-time X-ray powder diffraction. *Journal of the American Oil Chemists' Society*, 76(6), 669–676.
13. Malssen, Peschar, R., Brito, C., & Schenk, H. (1996). Real-time x-ray powder diffraction investigations on cocoa butter. III. Direct beta-crystallization of cocoa butter: occurrence of a memory effect. *Journal of the American Oil Chemists' Society*, 73(10), 1225–1230.
14. Marangoni, & Wesdorp, L. H. (2013). *Structure and properties of fat crystal networks* (2nd ed.). CRC Press.
15. Cuevas-Diarte, & Oonk, H. A. J. (2021). *Molecular mixed crystals* (Cuevas-Diarte & H. A. J. Oonk, Eds.). Springer.
16. Garti, & Widlak, N. R. (2012). Polymorphism and Mixing Phase Behavior of Major Triacylglycerols of Cocoa Butter. In *Cocoa Butter and Related Compounds* (pp. 1–1). AOCS Press.
17. Sato, Bayés-García, L., Calvet, T., Cuevas-Diarte, M. À., & Ueno, S. (2013). External factors affecting polymorphic crystallization of lipids. *European Journal of Lipid Science and Technology*, 115(11), 1224–1238.
18. Garti, & Satō, K. (2001). *Crystallization processes in fats and lipid systems* (Garti & K. Satō, Eds.; First edition.). CRC Press, an imprint of Taylor and Francis.
19. Wille, & Lutton, E. S. (1966). Polymorphism of cocoa butter. *Journal of the American Oil Chemists' Society*, 43(8), 491–496.
20. Bresson, Rousseau, D., Ghosh, S., Marssi, M. E., & Faivre, V. (2011). Raman spectroscopy of the polymorphic forms and liquid state of cocoa butter. *European Journal of Lipid Science and Technology*, 113(8), 992–1004.
21. Giacovazzo. (2011). *Fundamentals of crystallography* (3rd ed.). Oxford University Press.
22. Nogueira, Castiglioni, C., & Fausto, R. (2020). Color polymorphism in organic crystals. *Communications Chemistry*, 3(1), 34–34.
23. Menczel, & Grebowicz, J. (2023). *Handbook of Differential Scanning Calorimetry: Techniques, Instrumentation, Inorganic, Organic and Pharmaceutical Substances*. Elsevier Science & Technology.

